

AN INVESTIGATION OF THE MECHANICAL BEHAVIOR OF
BICOMPONENT FIBERS THROUGH THE USE OF MODELS

by

SANDRA LENSCH CUNNINGHAM

Submitted in Partial Fulfillment
of the Requirements for the
Degree of Bachelor of Science
at the
MASSACHUSETTS INSTITUTE OF TECHNOLOGY
September, 1963

Signature of Author..

Department of Mechanical Engineering, August 23, 1963

Certified by . . .

✓

Accepted by . . .

✓

Chairman, Departmental Committee on Theses

TABLE OF CONTENTS

	Page
I. Abstract.....	1
II. Introduction.....	2
III. Preparation of the Models.....	4
IV. Experimental Procedure.....	5
V. Discussion.....	6
VI. Appendix I.....	13
VII. Appendix II.....	20
VIII. Bibliography.....	32

ABSTRACT

The most important variables affecting the behavior of a bicomponent fiber are its cross sectional shape and the differential length change applied to crimp the fiber. These determine the fundamental radius of curvature and the configuration that a fiber attains as a result of varying environmental conditions. A helical coil configuration is predicted by the bimetallic analysis of a bicomponent fiber. However, with the application of different environmental constraints reversals of these helices are sometimes noted. This occurs to a great extent when the ratio of bending rigidities in the plane of the coil and transverse to this plane are very low. When this ratio is large, reversals seldom occur unless they are necessary for the shedding of torsional energy.

The presence of reversals in a fiber that is one of a group of fibers makes the assembly appear bulkier because they prohibit the fiber from twining with the other fibers to a great extent. The presence of reversals is desirable in fibers if a soft bulky yarn is desired.

INTRODUCTION

In recent years there has been an attempt to develop man-made fibers which will emulate the behavior of wool which is unique in the field of natural fibers. The high degree of crimp in a wool fiber gives it unique tactile properties. It has live behavior in finishing. And most important, wool has a high degree of bulk resulting from its three-dimensional structure. Since the bulk of wool varies as the crimp, attempts have been made to develop crimped man-made fibers.

Crimp in wool is a result of growth in a twisted follicle. Horio and Kondo [3] have shown that wool fibers have a definite bilateral structure that causes them to be crimped.

Attempts have been made to develop a similar bilateral structure in synthetic fibers in the hope that this would lead to the development of a man-made fiber combining the properties of synthetic fibers and the characteristics typical of wool.

Sisson and Morehead [4,5] produced crimped rayon by the two component approach. The bilateral character of the fibers produced crimp, but not aesthetic properties on the same order of magnitude as wool.

Recently a bilateral structure has been developed in an acrylic fiber which is marketed under the name Orlon-Sayelle¹ [2]. The fiber has a dog bone shaped cross section. Crimp is easily developed in this fiber because one side of the fiber shrinks more

1 Du Pont's registered trademark for its bicomponent fiber.

under heat than does the other. It develops into a highly three-dimensional spiral. This can be done in typical processing operations such as boil-off or dyeing procedures followed by drying. This crimped acrylic fiber shows a wool-like hand unusual in acrylic fibers and great elasticity.

The following investigation is a study of individual bilateral or bicomponent fibers through the use of bicomponent rubber models. An attempt has been made to investigate the affect of variables in the structure of the fiber on the crimp and on the behavior of the fiber under varying experimental conditions.

Preparation of the Models

The first models were made of gum rubber that was cut from a $\frac{1}{4}$ inch thick sheet in strips three feet long and $\frac{1}{2}$ inch wide. These models were discarded as unsuitable because they were too large to handle easily and because the glue did not bond the strips together well.

The models used for the bulk of the experiment and the photographs were made from custom-cut strips of neoprene rubber. The ten foot long strips were obtained with two cross sections, $1/8$ " x $1/4$ " and $1/16$ " x $1/2$ ". The models were made by gluing the strips together with neoprene glue. Three basic cross sections were used: Square, T-shaped, and ribbon. The length differential between the strips that gives the specimen crimps was easily introduced in manufacture. One of the strips was stretched out until it was strained to .2, .3, or .4, depending upon the specimen desired. It was then nailed to the floor. The other strip, the unstretched one, was also nailed to the floor at this time because this made it easier to apply the glue. Two coats of glue were applied to the strips. The unstretched piece was then laid on the stretched piece, and pressure was applied until a bond formed between the two strips. The models were allowed to dry for several hours. Then without releasing the model from being nailed to the floor, the unstretched part of the model was painted with white paint so that the model would photograph better. The models were then allowed to dry for several days undisturbed.

EXPERIMENTAL PROCEDURES

The force versus normalized length curves were obtained from experiments run on the Instron. For this, the models were forced into the desired forms, i.e. all coils or all reversals, then they were clamped in the jaws so that they could not rotate or strings attached to their ends were clamped in the jaws so that the ends could rotate depending upon the trial. Force-deflection data was taken.

For more qualitative observations and for the photographs, there were the following basic procedures:

1. The model(s) was straightened and then allowed to contract with the ends restrained from rotation.
2. The model(s) was straightened and then was allowed to contract while being held by strings attached to the ends of the model so that the ends were free to rotate.
3. The model was swung and shaken randomly with another model.

The resulting configurations were noted.

DISCUSSION OF FINDINGS

The mechanical shape of the cross section and the differential length change between the two components are the most significant factors determining the behavior of the bicomponent fiber.

The equilibrium curvature is a function of the bending rigidity of the model and the differential length change. Using Timoshenko's [6] bimetallic thermostat analogy of fiber crimp assuming (1) the materials obey Hooke's law of elasticity, (2) both strips are the same unit width W , (3) the cross section of the strip is rectangular, and (4) the radius of curvature is much greater than the thickness of the bimetallic strip, the relation between the equilibrium curvature and the mechanical shape and differential length change can be expressed by the equation:

$$K_0 = \frac{1}{\rho_0} = \frac{6 \frac{a_1}{a_2} \left(1 + \frac{a_1}{a_2}\right)^2 \frac{\Delta L}{L}}{h \left[\frac{E_1}{E_2} + 4 \frac{a_1}{a_2} + 6 \left(\frac{a_1}{a_2}\right)^2 + 4 \left(\frac{a_1}{a_2}\right)^3 + \frac{E_2}{E_1} \left(\frac{a_1}{a_2}\right)^4 \right]}$$

This should be modified, however, because (1) both strips are not the same unit width W , (2) the cross sections of all of the strips are not rectangular, and (3) the radius of curvature for some of the strips is nearly the same order of magnitude as the thickness of the bicomponent strip.

Brand and Backer [1] derived a more realistic equation following Timoshenko's analysis, but avoiding assumptions (2) and (3) although retaining the assumption

implicit in a rectangular cross section that the distance between the centroids d_1 and d_2 is equal to $\frac{1}{2}$ the diameter of the total sections A_1 and A_2 . This equation is:

$$K_o = \frac{1}{\rho_o} = \frac{\Delta L/L}{\frac{h}{2} + \frac{h}{2} \left[I_1 \left(\frac{1}{A_1} + \frac{E_1}{E_2 A_2} \right) + I_2 \left(\frac{1}{A_2} + \frac{E_2}{E_1 A_1} \right) \right]}$$

This equation was used to calculate the radii for the models. However, the actual radii did not agree.

CROSS SECTION	THEORETICAL		ACTUAL	
	$\Delta L/L = .3$	$\Delta L/L = .4$	$\Delta L/L = .3$	$\Delta L/L = .4$
SQUARE	$\rho_o = .425$ in.	$\rho_o = .32$ in.	$\rho_a = .815$ in.	$\rho_a = .685$ in.
T-SHAPED	$\rho_o = .314$ in.		$\rho_a = .56$ in.	
RIBBON	$\rho_o = .208$ in.	$\rho_o = .156$ in.	$\rho_a = .375$ in.	$\rho_a = .3125$ in.

The actual radii are consistently roughly twice as large as the theoretical radii. Perhaps a modification of the Brand-Backer result

$$K_o = \frac{1}{\rho_o} = \frac{\Delta L/L}{h + h \left[I_1 \left(\frac{1}{A_1} + \frac{E_1}{E_2 A_2} \right) + I_2 \left(\frac{1}{A_2} + \frac{E_2}{E_1 A_1} \right) \right]}$$

is more correct for the range of differential length change used for the models in this thesis.

A helical coil configuration is predicted by the bimetallic analysis of a bicomponent fiber. However, with the application of different environmental constraints, reversals of these helices are sometimes noted.

Photo Plate 1 shows the formation of a reversal in six stages. The model was firmly clamped in the jaws of the Instron so that it could not rotate. Notice that the section in the center that forms the reversal rotates so that the helical coils can form above and below it. In this way it serves to shed torsional energy. Unlike the helical coils, the reversal is bent in the transverse plane. As can be seen from graphs 1 and 2, a reversal stores more energy than a corresponding helical coil. Graph 1 shows the energy as calculated from a mathematical treatment of the helical coil model with a square cross section and $\Delta L/L = .3$. Graph 2 shows the energy as calculated from measurements taken from a reversal in a model with square cross section and $\Delta L/L = .3$.

Simple tests were run on the Instron to get force vs. normalized length curves for helical coils and reversals in a model with square cross section and $\Delta L/L = .3$ and $\Delta L/L = .4$. There was little difference observed between the area under the curves for the reversals and helices; the curves practically coincide, see GRAPHS 3,4, AND 5.

In the case of the square cross section, the ratio of the bending rigidities is one. If one straightens the model and then allows it to contract with the ends

restrained from rotation, several configurations may result. Sometimes the model becomes all reversals. More often there are both helical coils and reversals in the resulting configuration. With this cross section, the proportion of reversals to helical coils is high. A single model will usually attain the same equilibrium configuration in successive trials. If the model is straightened, and allowed to contract with the ends free to rotate, there is little difference in the equilibrium configuration.

The ratio of the bending rigidities for the T-shaped cross section is 4.3. This model is more restrained in its mobility than the square cross section model. When the model is straightened and allowed to contract with both ends restrained from rotation, fewer reversals develop than in the similar case with the square cross section. However, if the ends are free to rotate, only one or two reversals in a five foot length of this model will occur. The ends of the model will rotate until most of the reversals near the ends have been shed.

The ratio of bending rigidities for the models with the ribbon cross section is 16. When these models are straightened and then allowed to contract with both ends being restrained from rotation, one or two form along the length of the specimen; the rest of the model becomes helical coils. Most of the torsional energy is shed creating the reversals. When a model was straightened and allowed to contract with both ends free to rotate, a perfectly helical configuration often resulted. Reversals were more likely to form in the models with small $\Delta L/L$'s. Reversals in these models can have smaller curvature in the transverse plane and yet join up with the helical coils on either side. The

larger the curvature required in the transverse plane; the less likely the formation of a reversal.

Therefore, the most important factors in the behavior of a bicomponent fiber are its mechanical shape cross section and the differential length change. These determine the radius of the helical coil it can coil into and determine the fiber's behavior under varying environmental constraints. A large $\Delta L/L$ results in a tightly crimped fiber with little tendency to have reversals. A large bending rigidity in the transverse plane compared to that in the bending plane of the coil reduces the tendency to have reversals. When the bending rigidities are of the same order of magnitude, reversals will be formed easily and serve to shed torsional energy (see graph 6) such as for the case where a straightened model (of square cross section and $\Delta L/L=3$) is allowed to contract with out rotation of the ends. Two equilibrium configurations are proposed. The section could have ten helical coils (actually physically impossible) or it could have nine helical coils and one reversal. The graph shows that case two would be the more stable configuration. For a ribbon cross section, Graph 7 shows that the section with all helical coils requires more energy than the similar case with helical coils with one reversal. Unlike the previous case, the energy difference is considerable.

We should consider how the models behave in groups. Specifically, we should consider the significance of the presence of a reversal as compared to that of a coil. Which configuration will be more desirable for a fiber? Also, we should investigate how fibers with different crimp frequency and amplitude behave in mixed groups.

Photos G through L on Photo Plate 3 show the models representing fibers in groups of two: G and H show two fibers of square cross section with . They had been straightened out separately and then allowed to contract together, the ends being restrained from rotation. Notice that each model has both helical coils and reversals. The helical coils of one model try to match and follow the coils on the other model so that they entwine. The reversals do not twine with the coils or with corresponding reversals. They make the assembly appear bulkier. In I, a model with $\Delta L/L = .3$ and a model with $\Delta L/L = .4$ are shown in the configuration reached after being randomly shaken together. The helical coil parts of each fiber still try to follow and twine together, but since the crimp frequencies of the models are different there is considerable mismatch.

J, K, and L show two models .3's, .4's, and a .3 and .4 respectively, that have been just pushed up against each other. The configurations of the models interfere and there is no matching..

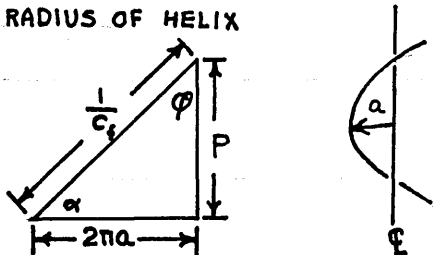
A, B, and C of Photo Plate 2 show groups of three models of square cross section with $\Delta L/L = .3$. The helical sections still twine well, and the reversals add bulk. If you compare A, B, and C with the group D, E, and F which are of two models with $\Delta L/L = .3$ and one model with $\Delta L/L = .4$, you will notice that the groups in D, E, and F seem bulkier than those in A, B, and C. The models with $\Delta L/L = .3$ are not able to twine with the model with $\Delta L/L = .4$. The presence of the model with $\Delta L/L = .4$ hinders the models with $\Delta L/L = .3$ from twining with each other. This encourages the development of reversals in the models with $\Delta L/L = .3$.

From this we can conclude that the presence of reversals in a fiber gives bulkiness to an aggregate of fibers and that the presence of fibers with different crimp frequencies and amplitudes leads to the formation of reversals which contribute to the bulkiness of a group of fibers.

APPENDIX I

SYMBOLS, DEFINITIONS, AND FORMULAS FOR BICOMPONENT MODEL

SYMBOL	MTL UNITS	DEFINITION OR DESCRIPTION	FORMULAS
C_f	L^{-1}	CRIMP FREQUENCY, NUMBER OF CRIMPS PER EXTENDED LENGTH	$\frac{C_n}{L} ; C_f = \frac{K_0}{2\pi} = \frac{1}{2\pi\rho_0}$ $C_f = \frac{\sqrt{C_i(2-C_i)}}{2\pi a}$
C_n		NUMBER OF CRIMPS IN A GIVEN FIBER SECTION	
L	L	EXTENDED LENGTH OF THE FIBER SECTION OVER WHICH C_n WAS COUNTED	
K_0	L^{-1}	FUNDAMENTAL CURVATURE DUE TO "BIMETALLIC" ACTION (DIFFERENTIAL LENGTH CHANGE ΔL)	$K_0 = 2\pi C_f ; K_0 = 1/\rho_0$ $K_0 = \frac{\Delta L/L}{\frac{h}{2} + \frac{h}{2} \left[I_1 \left(\frac{1}{A_1} + \frac{E_1}{E_2 A_2} \right) + I_2 \left(\frac{1}{A_2} + \frac{E_2}{E_1 A_1} \right) \right]}$ <p>SUBSCRIPTS REFER TO THE COMPONENTS 1 AND 2 OF THE BICOMPONENT FIBER 1 = HIGH SHRINKAGE SIDE</p>
A	L^2	AREA OF CROSS SECTION	
h	L	DEPTH OF CROSS SECTION ALONG THE RADIUS OF CURVATURE OF THE FIBER AT RIGHT ANGLES TO THE NEUTRAL AXIS OF BENDING	
ΔL	L	DIFFERENCE IN LONGITUDINAL LENGTH CHANGE OF THE TWO COMPONENTS OF A BICOMPONENT FIBER AS A RESULT OF CHANGE IN ENVIRONMENT.	
ρ_0	L	FUNDAMENTAL RADIUS OF CURVATURE DUE TO "BIMETALLIC" ACTION (ΔL)	
E	$ML^{-1}T^{-2}$	ELASTIC MODULUS (IN TENSION)	
C_i		CRIMP INDEX	$C_i = 1 - \frac{\rho}{L} = 1 - \sqrt{1 - (K_0 a)^2} = (1 - \rho C_f)$ $C_i = 1 - \sqrt{1 - 4\pi^2 a^2 C_f^2}$

a	L	RADIUS OF HELIX 	$a = \frac{\sqrt{C_i(2-C_i)}}{2\pi C_f}$
P	L	CRIMP PERIOD	$P = \frac{\sqrt{1-(2\pi a C_f)^2}}{C_f} = \frac{1-C_i}{C_f}$
K	L^{-1}	CURVATURE OF A HELIX	$K = \frac{\sin^2 \phi}{a} ; K = K_0^2 a$
t	L^{-1}	TORSION IN A HELIX	$t = \frac{\sin \phi \cos \phi}{a} = K_0 \sqrt{1-(K_0 a)^2}$
R_λ		RIGIDITY RATIO	$R_\lambda = \frac{EI}{GI_p} = 1 + \frac{1}{2\pi C_f + \frac{d}{\theta}(1-C_i) - C_i(2-C_i)}$
I_p	L^4	MOMENT OF INERTIA OF AREA (A) IN TORSION ABOUT AXIS \perp TO (A)	
d	L	AMOUNT OF EXTENSION OF CRIMPED FIBER LENGTH	
θ		AMOUNT OF ROTATION OF THE FREE END WHEN EXTENDING A PERFECT HELICALLY CRIMPED FIBER AT ONE END ONLY.	$\theta = PaL \sin \alpha \cos \alpha \left(\frac{1}{GI_p} - \frac{1}{EI} \right)$

CALCULATION OF THE FUNDAMENTAL RADIUS OF CURVATURE
DUE TO "BIMETALLIC" ACTION

The fundamental radius of curvature was calculated using the relation derived by Brand and Backer using Timoshenko's analysis but avoiding the assumptions that both strips are the same unit width W and that the cross section of the strip is rectangular, but retaining the assumption implicit in a rectangular cross section that the distance between the centroids is equal to one half the diameter of the total sections A_1 and A_2 .

$$\rho_o = \frac{\frac{h}{2} + \frac{h}{2} \left[I_1 \left(\frac{1}{A_1} + \frac{E_1}{E_2 A_2} \right) + I_2 \left(\frac{1}{A_2} + \frac{E_2}{E_1 A_1} \right) \right]}{\Delta L/L}$$

where the subscript 1 refers to the strained strip and the subscript 2 refers to the unstrained strip

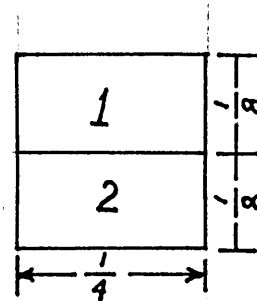
SQUARE CROSS SECTION :

$$h = \frac{1}{4} \text{ inch}$$

$$I_1 = I_2 = 1.63 \times 10^{-4} \text{ inch}^4$$

$$A_1 = A_2 = \frac{1}{32} \text{ in.}^2$$

$$E_1 = E_2$$



For $\Delta L/L = .3$

$$\rho_o = .425 \text{ in.}$$

$$\rho_o = .815 \text{ in.}$$

ACTUAL

FOR $\Delta L/L = .4$

$$\rho_o = .32 \text{ in.}$$

$$\rho_o = .685 \text{ in.}$$

ACTUAL

T-SHAPED CROSS SECTION:

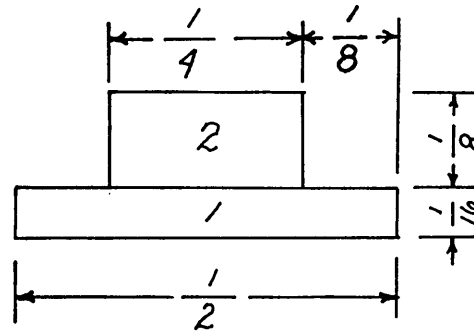
$$h = \frac{3}{16} \text{ in.}$$

$$I_1 = 7.92 \times 10^{-5} \text{ in.}^4$$

$$I_2 = 10.97 \times 10^{-5} \text{ in.}^4$$

$$A_1 = A_2 = \frac{1}{32} \text{ in.}^2$$

$$E_1 = E_2$$



$$\Delta L/L = .3$$

$$\rho_o = .314 \text{ in.}$$

$$\rho_o = .56 \text{ in.}$$

ACTUAL

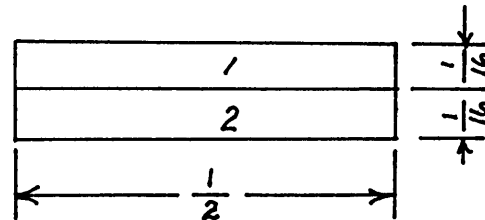
RIBBON CROSS SECTION:

$$h = \frac{1}{8} \text{ in.}$$

$$I_1 = I_2 = 4.08 \times 10^{-5} \text{ in.}^4$$

$$A_1 = A_2 = \frac{1}{32} \text{ in.}^2$$

$$E_1 = E_2$$



FOR $\Delta L/L = .3$

$$\rho_o = .208 \text{ in.}$$

$$\rho_o = .375 \text{ in.}$$

ACTUAL

FOR $\Delta L/L = .4$

$$\rho_o = .156 \text{ in.}$$

$$\rho_o = .3125 \text{ in.}$$

ACTUAL

CALCULATION OF BENDING RIGIDITIES

SQUARE CROSS SECTION:

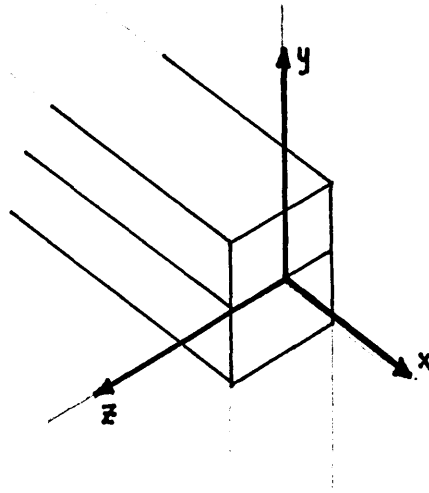
$$I_{yy} = \int_{-\frac{h}{2}}^{\frac{h}{2}} y^2 b \, dy = \frac{bh^3}{12}$$

$$I_{zz} = \int_{-\frac{b}{2}}^{\frac{b}{2}} z^2 h \, dz = \frac{hb^3}{12}$$

$$EI_{yy} = 3.26 \times 10^{-4} \text{ in.}^4 E$$

$$EI_{zz} = 3.26 \times 10^{-4} \text{ in.}^4 E$$

$$\frac{EI_{yy}}{EI_{zz}} = 1$$

T-SHAPED CROSS SECTION:

$$EI_{yy} = 1.89 \times 10^{-4} \text{ in.}^4 E$$

$$EI_{zz} = 8.15 \times 10^{-4} \text{ in.}^4 E$$

$$\frac{EI_{zz}}{EI_{yy}} = 4.3$$

RIBBON CROSS SECTION:

$$EI_{yy} = 8.16 \times 10^{-5} \text{ in.}^4 E$$

$$EI_{zz} = 1.3 \times 10^{-3} \text{ in.}^4 E$$

$$\frac{EI_{zz}}{EI_{yy}} = 16$$

ENERGY CALCULATIONS

If a fiber initially held in a straight configuration ($a = 0$; $C_i = 0$; twist = 0; helix curvature $K = 0$) is allowed to contract without allowing the ends to rotate, the strain energies per unit length for the model in bending U_b , and in torsion U_t , at any time will be given by:

$$U_b = \sum \frac{1}{2} EI (\Delta K)^2$$

$$U_t = \sum \frac{1}{2} GI_p (\Delta t)^2$$

The datum condition for calculation of the bending energy is that in which the helix is completely collapsed, and the curvature equals the fundamental curvature due to "bimetallic" action. In the case of a reversal, the datum curvature in the transverse plane is equal to zero. Then:

$$U_b = \frac{1}{2} I_{yy} E (K - K_0)^2 + \frac{1}{2} EI_{zz} (K_T - 0)^2$$

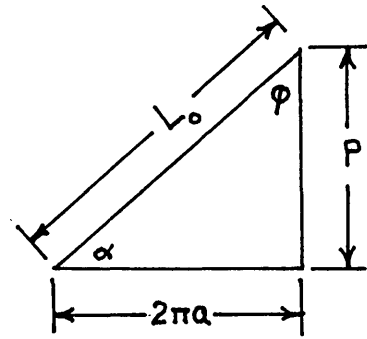
The datum condition for calculation of the torsional energy is that in which the model is completely straightened and the torsion equals K_0 .

Then:
$$U_t = \frac{1}{2} GI_p (t - t_0)^2$$

For a helical coil the energies can be calculated easily. The path of one crimp may be developed in a plane forming a right triangle. The hypotenuse is the extended length L_0 of this crimp loop. The distance between crimps p along the helix axis is one side of the triangle. The other side is equal to 2π times the helix radius a .

$$L_o^2 = p^2 + 4\pi^2 a^2$$

$$a = \sqrt{\frac{L_o^2 - p^2}{4\pi^2}}$$



$$\text{THEN } \kappa = \frac{\sin^2 \phi}{a} = \frac{\left(\frac{2\pi a}{L_o}\right)^2}{a} = \frac{2\pi}{L_o^2} \sqrt{L_o^2 - p^2}$$

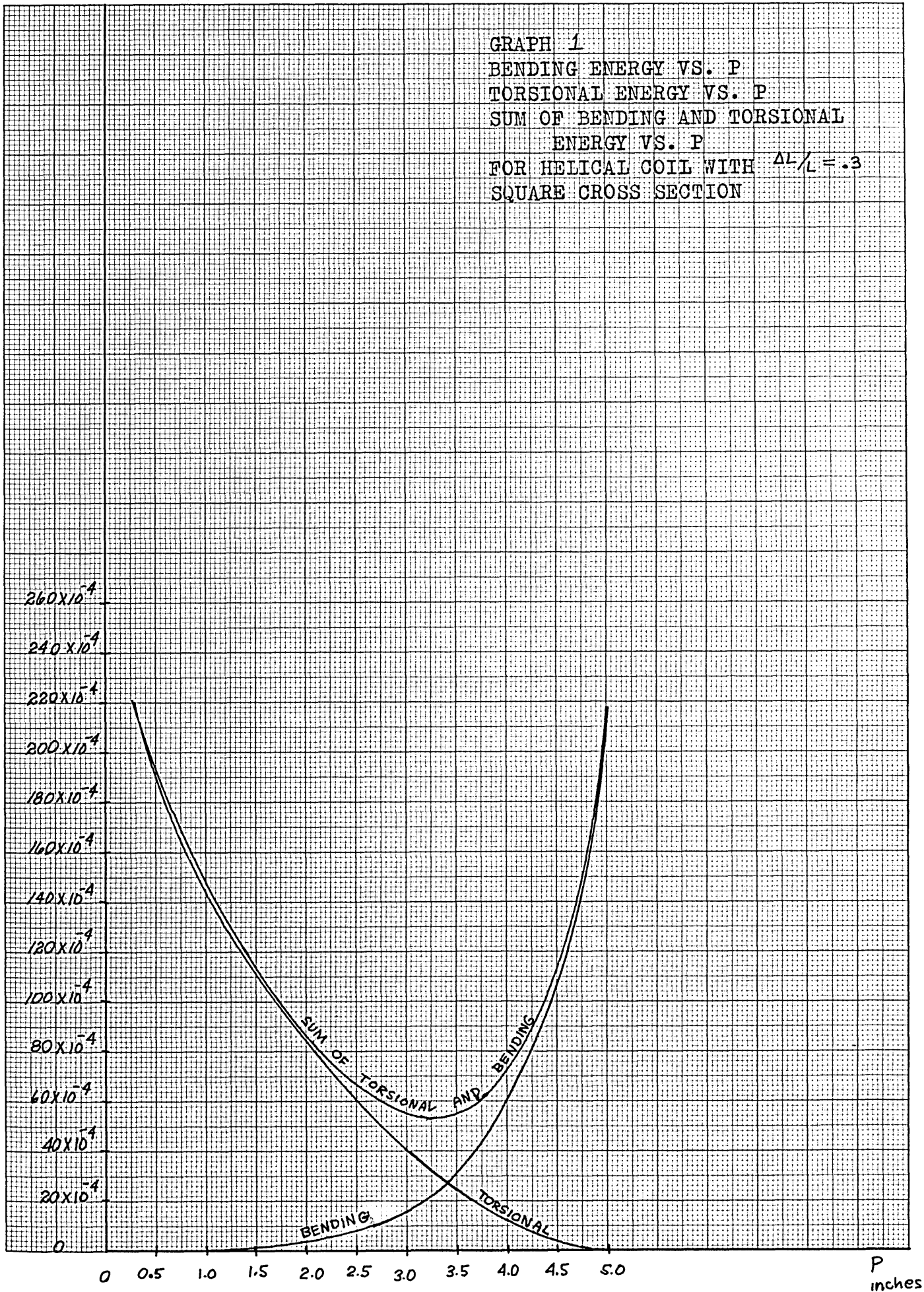
$$\text{AND } U_b = \frac{1}{2} EI_{yy} \left(\frac{2\pi}{L_o^2} \sqrt{L_o^2 - p^2} - K_o \right)^2$$

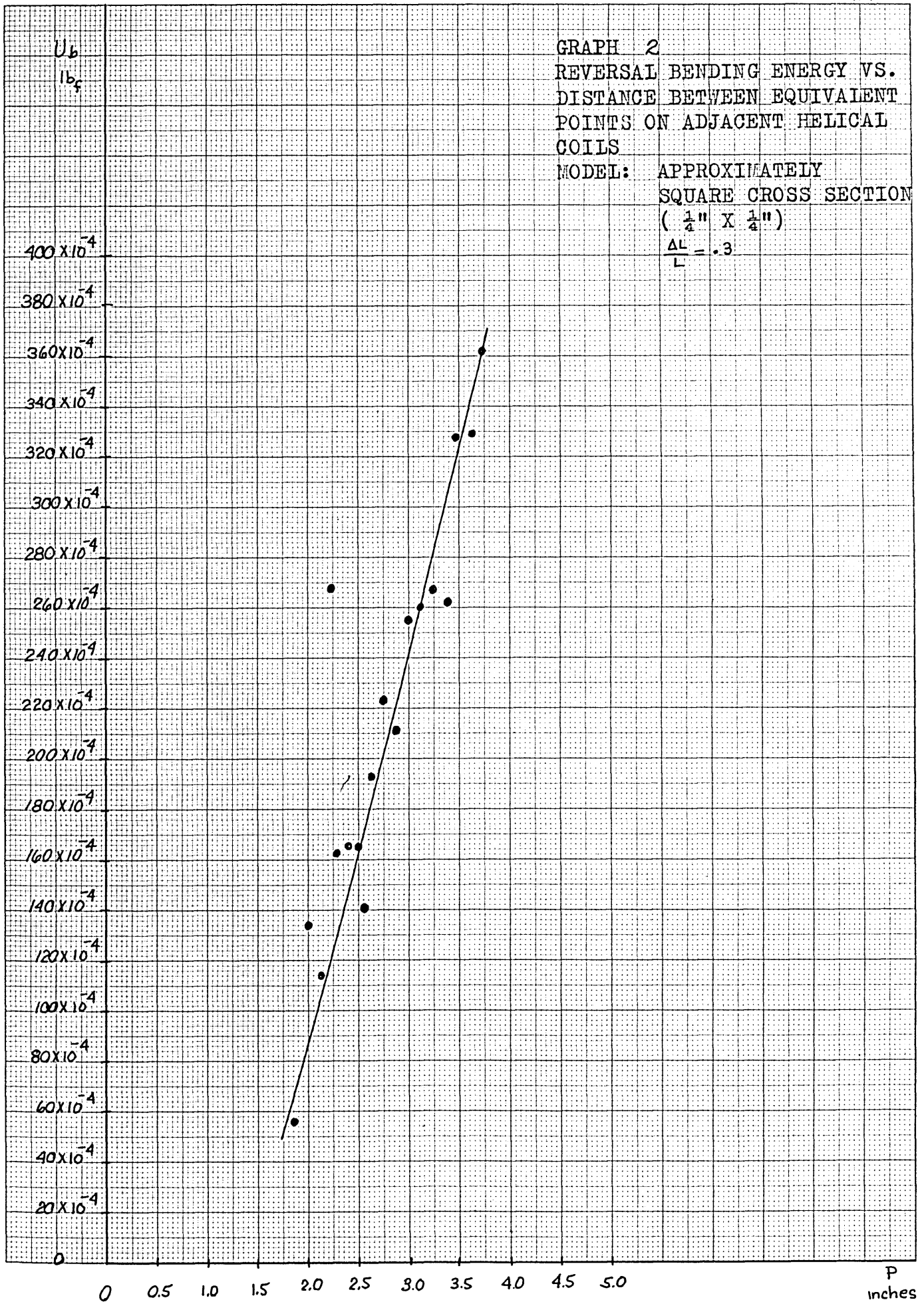
$$\text{ALSO } \tau = \frac{\sin \phi \cos \phi}{a} = \frac{\left(\frac{2\pi a}{L_o}\right) \left(\frac{p}{L_o}\right)}{a} = \frac{2\pi}{L_o^2} p$$

$$\text{THEN } U_t = \frac{1}{6} EI_p \left(\frac{2\pi}{L_o^2} p - K_o \right)^2$$

For a reversal, the energy can be calculated as a function of p , too, measuring the curvatures on a reversal and noting the value of p for adjacent helical coils. From this information, the amount of energy stored in a reversal under the same conditions can be calculated and compared.

GRAPH 1
 BENDING ENERGY VS. P
 TORSIONAL ENERGY VS. P
 SUM OF BENDING AND TORSIONAL
 ENERGY VS. P
 FOR HELICAL COIL WITH $\Delta L/L = .3$
 SQUARE CROSS SECTION





F
lbs.

NORMALIZED CURVE
FORCE VS. x/L_0

ENDS RESTRAINED FROM ROTATION
ALL REVERSALS
SQUARE CROSS SECTION WITH $\Delta^2/L_0 = .4$

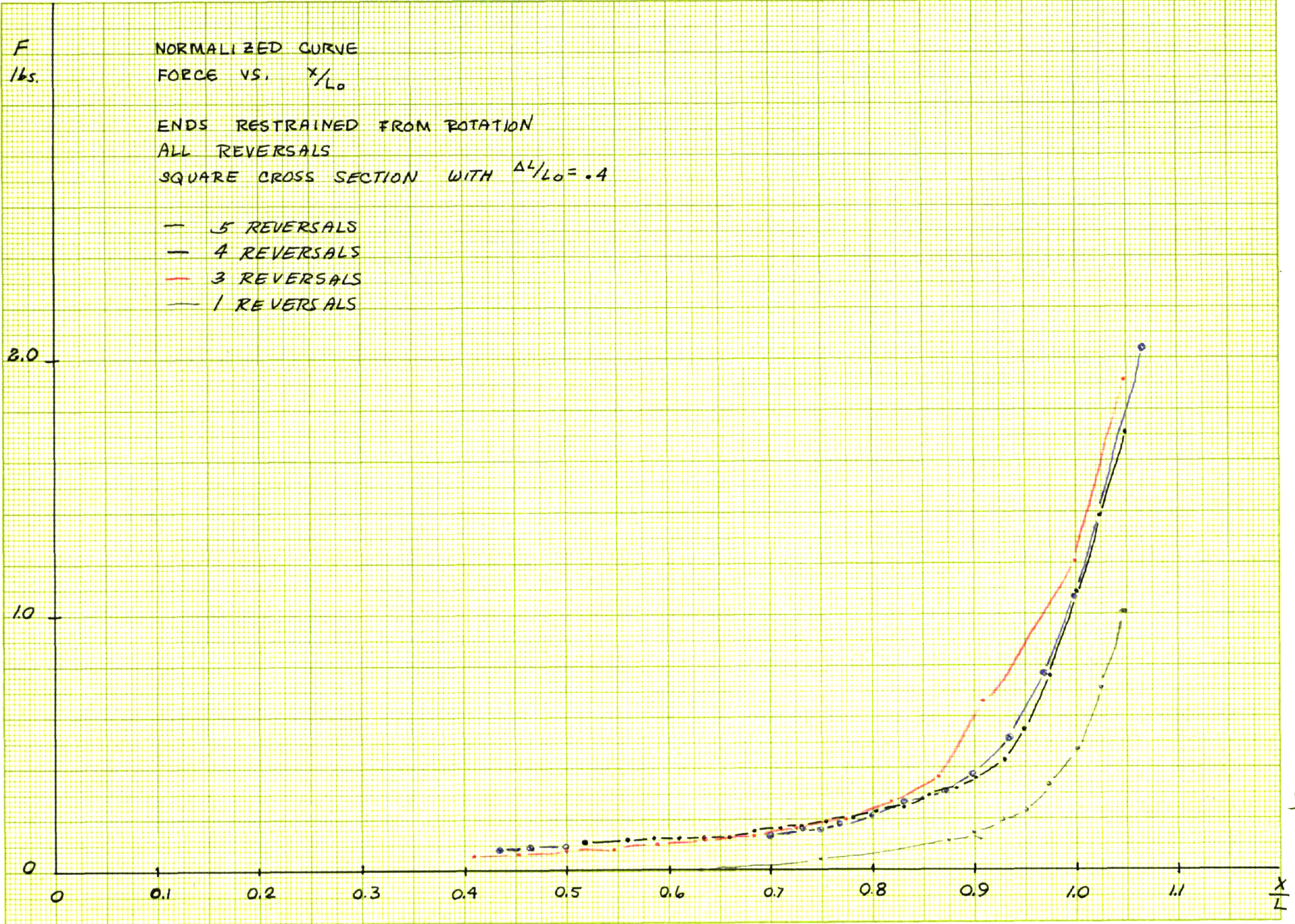
- 5 REVERSALS
- 4 REVERSALS
- 3 REVERSALS
- 1 REVERSALS

2.0

1.0

0

0 0.1 0.2 0.3 0.4 0.5 0.6 0.7 0.8 0.9 1.0 1.1 x/L



FORCE
POUNDS

GRAPH 4

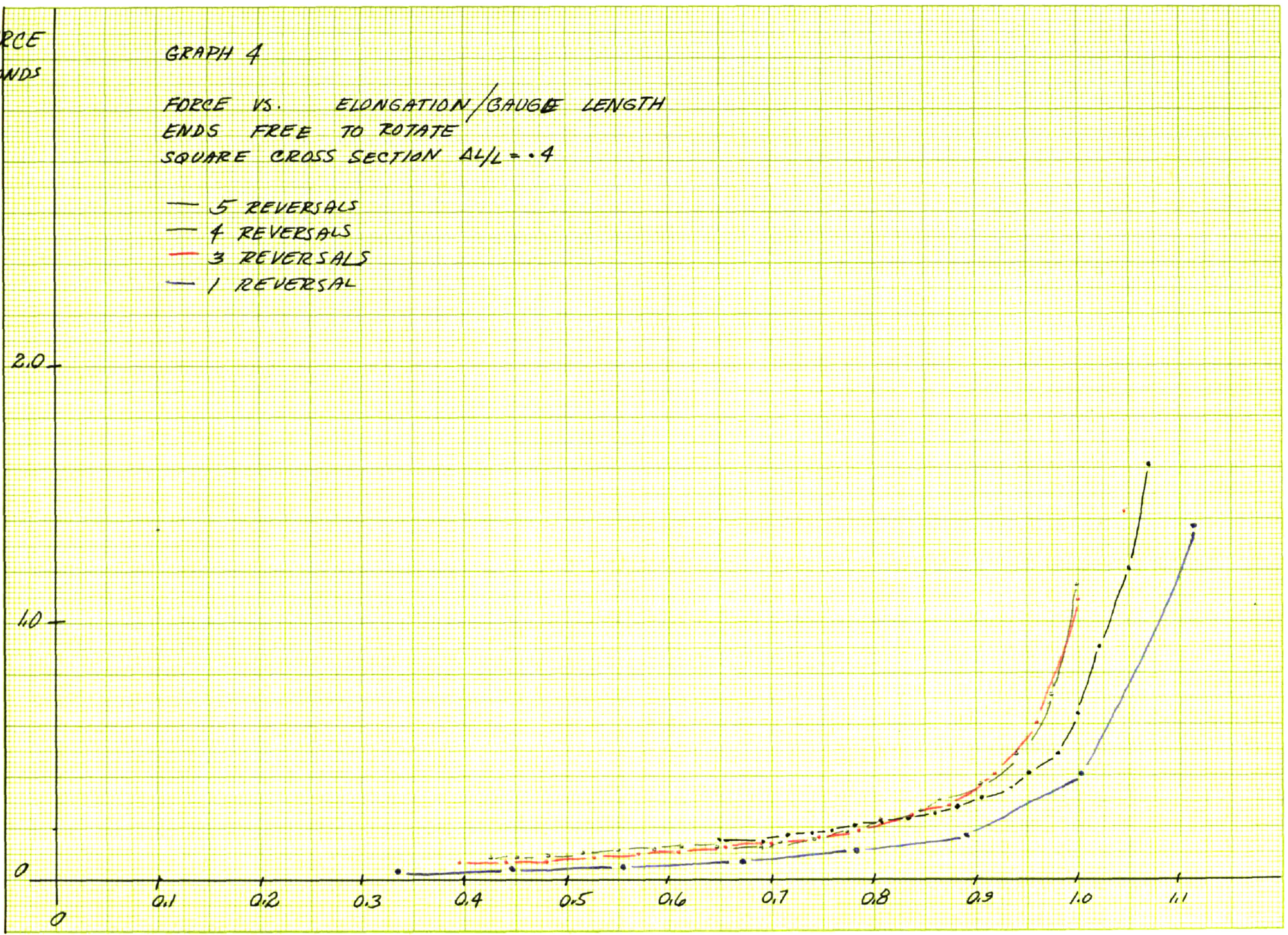
FORCE VS. ELONGATION/GAUGE LENGTH
ENDS FREE TO ROTATE
SQUARE CROSS SECTION $A/L = .4$

- 5 REVERSALS
- 4 REVERSALS
- 3 REVERSALS
- 1 REVERSAL

2.0

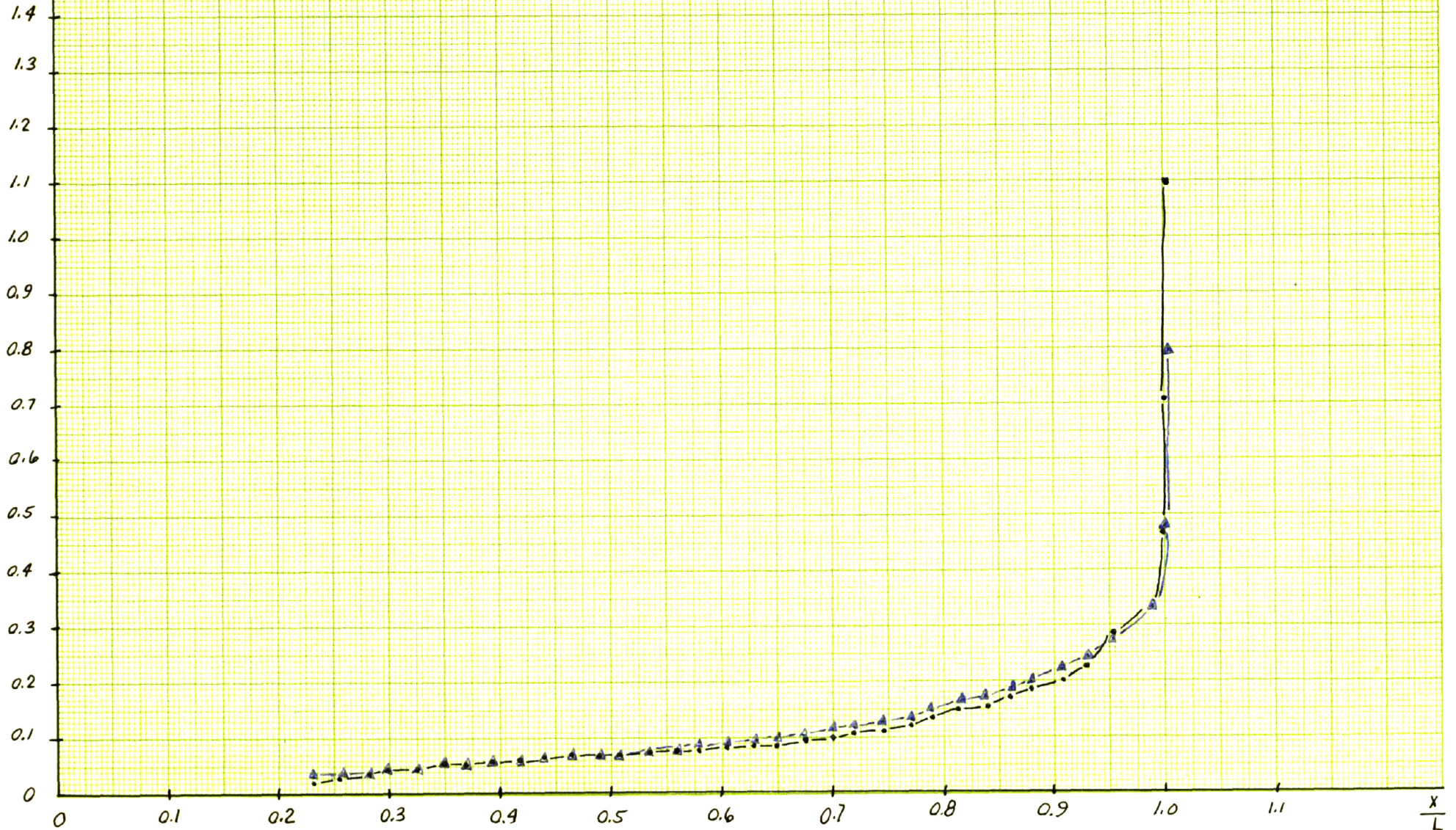
1.0

0

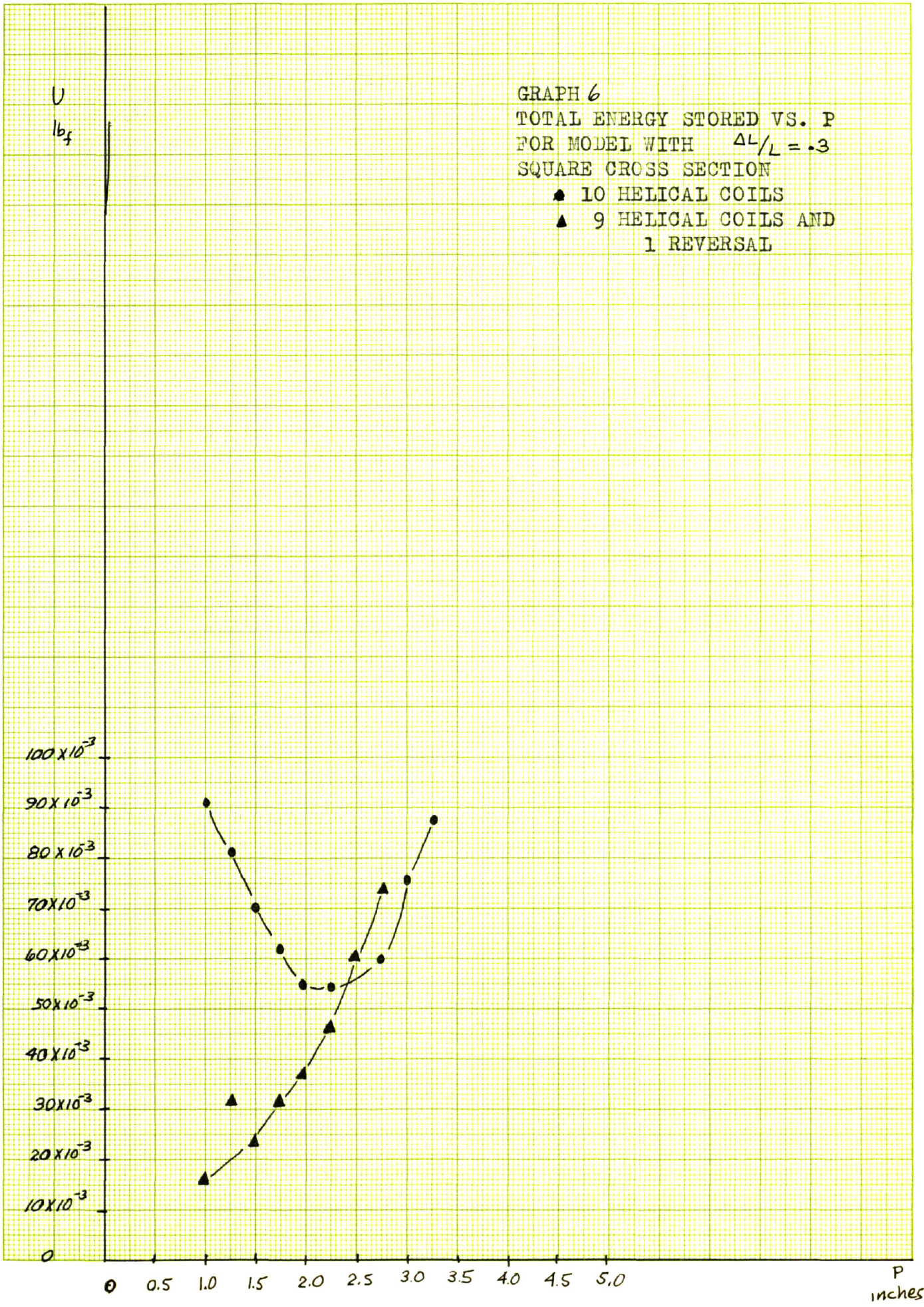


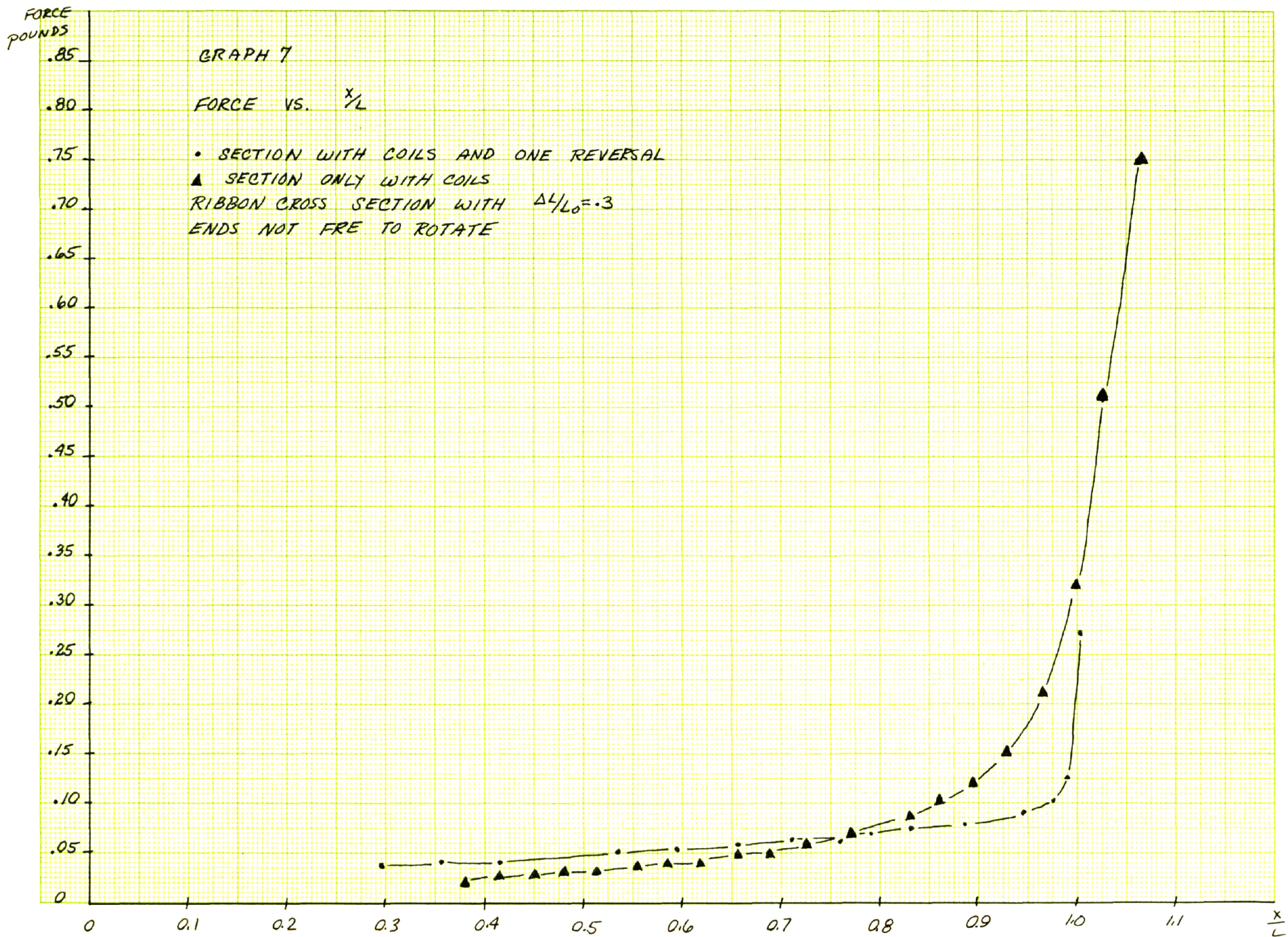
Force
lbs.

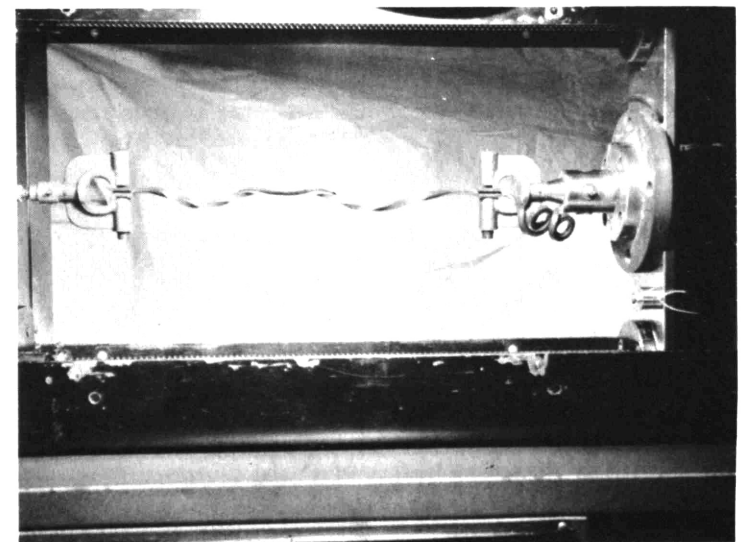
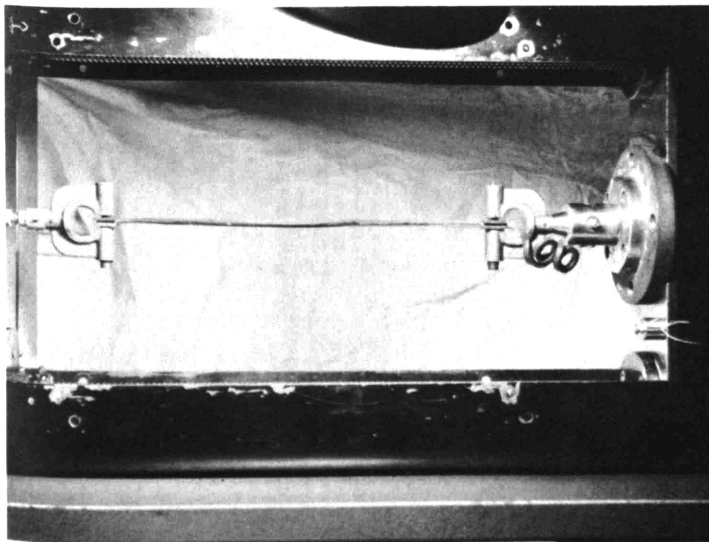
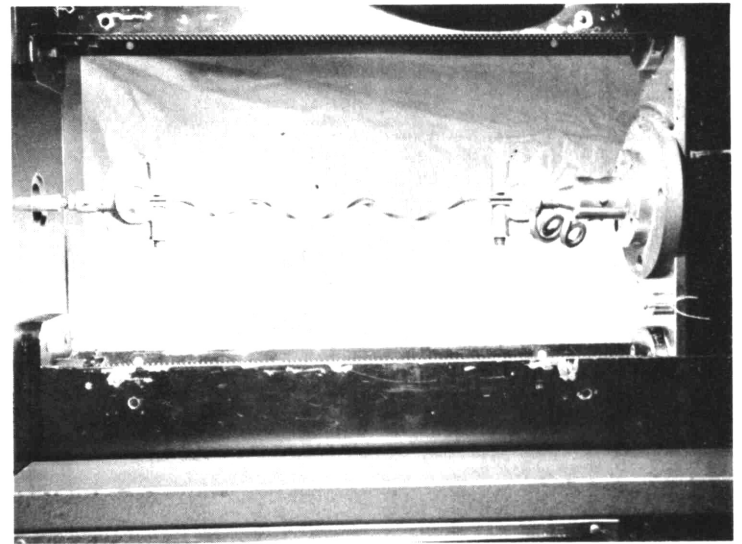
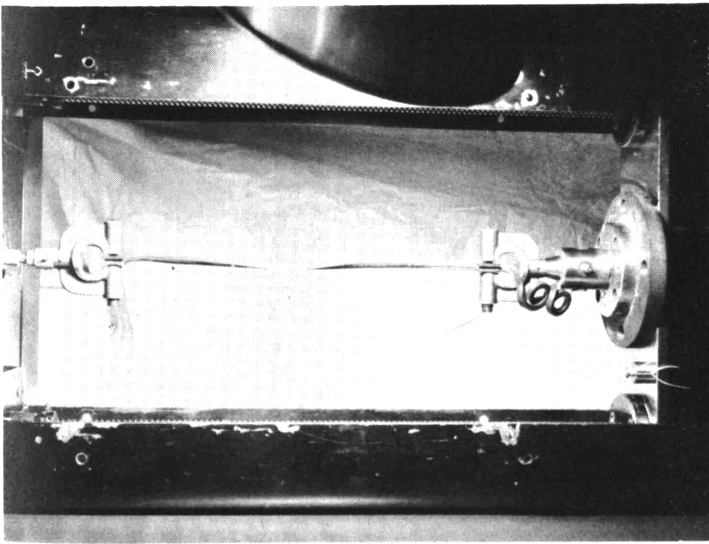
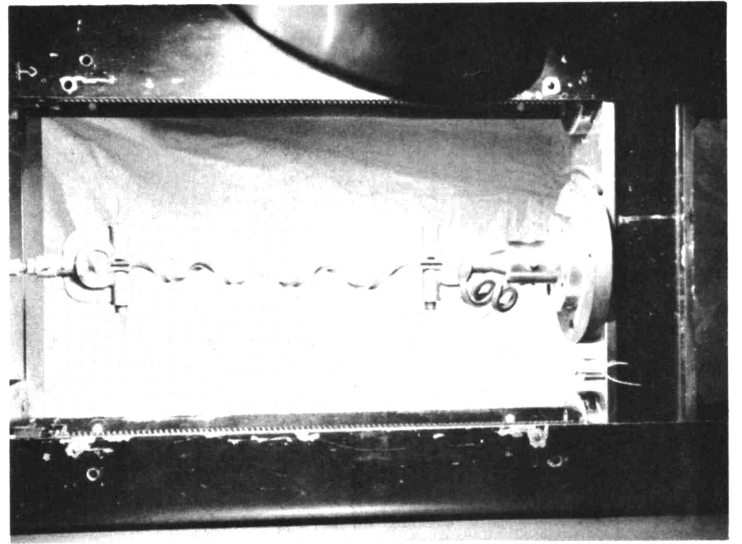
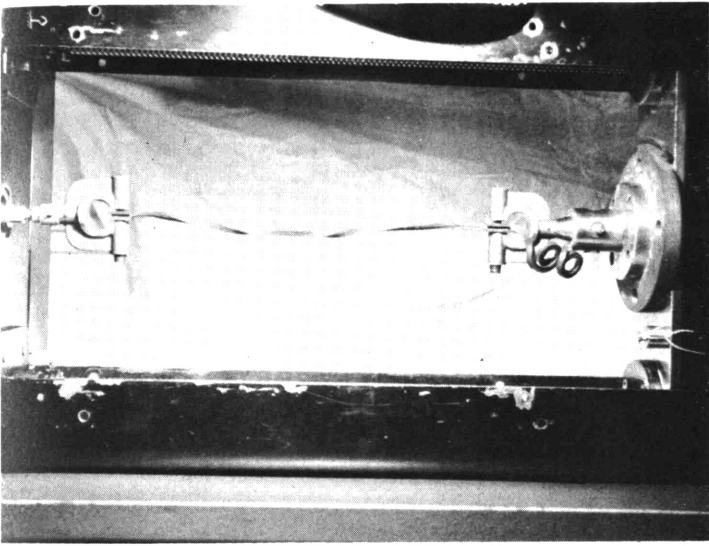
GRAPH 5 $\frac{\text{EXTENDED LENGTH}}{\text{SPECIMEN LENGTH}} = \frac{x}{L}$
FORCE VS. $\frac{x}{L}$
SQUARE CROSS SECTION $\Delta L/L = 0.3$
• SECTION WITH REVERSALS
▲ SECTION WITH HELICAL COILS
ENDS FREE TO ROTATE

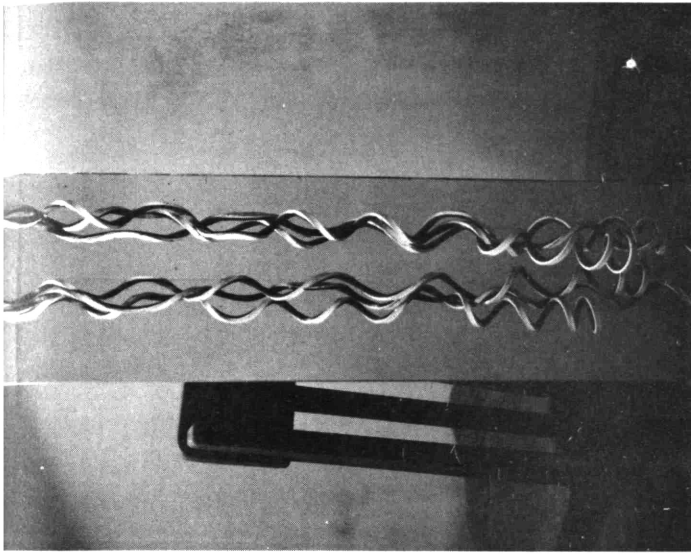


GRAPH 6
 TOTAL ENERGY STORED VS. P
 FOR MODEL WITH $\Delta L/L = .3$
 SQUARE CROSS SECTION
 ● 10 HELICAL COILS
 ▲ 9 HELICAL COILS AND
 1 REVERSAL

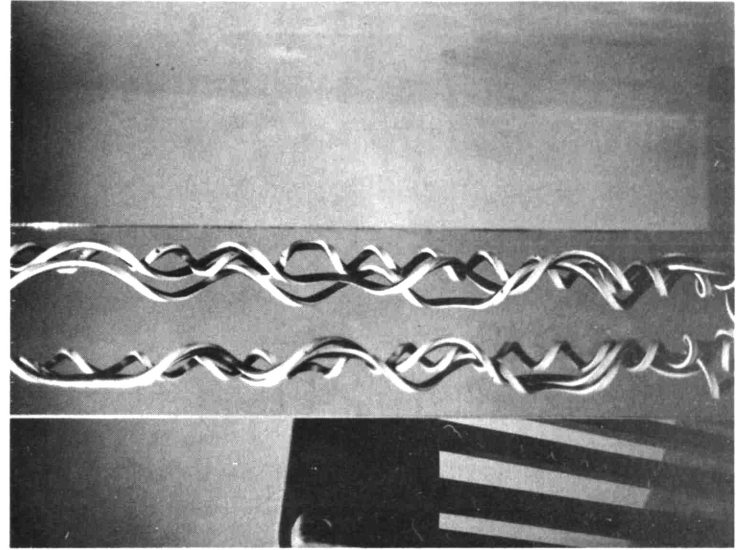




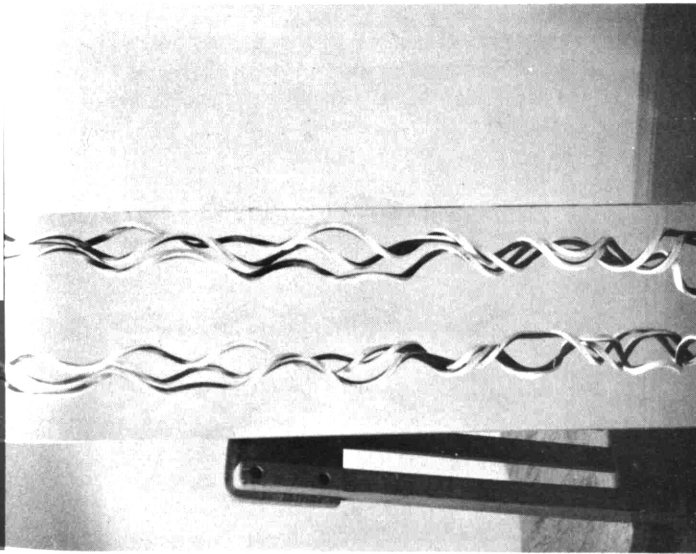




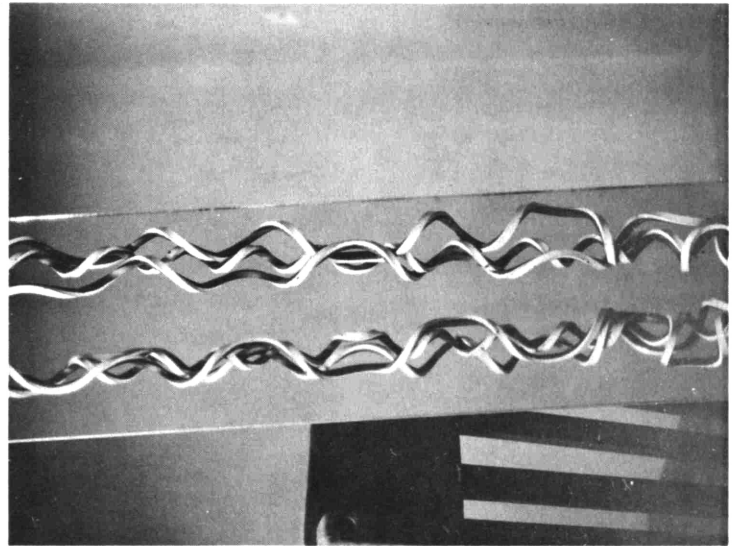
B. C.



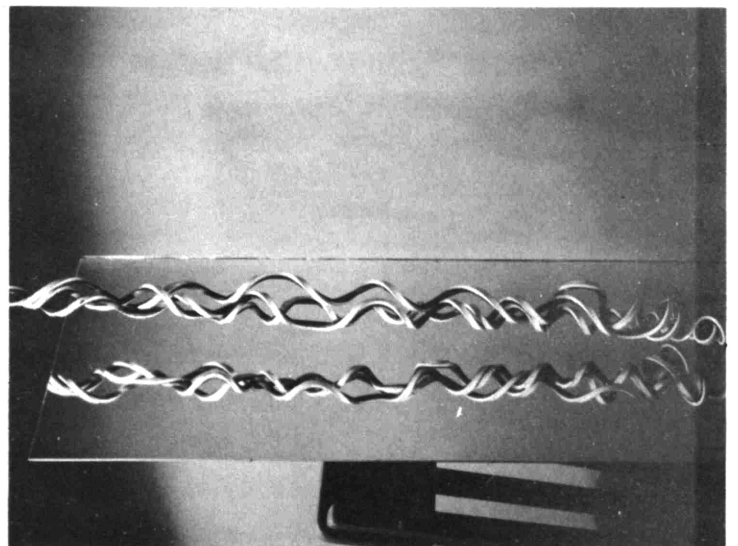
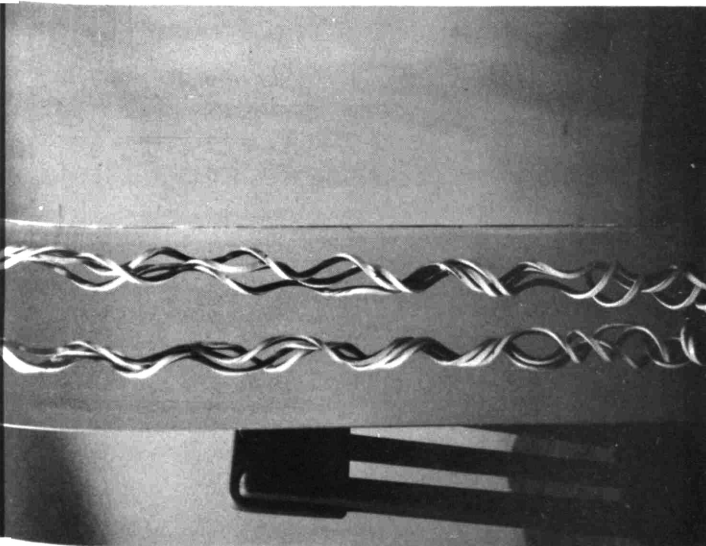
E.



A.

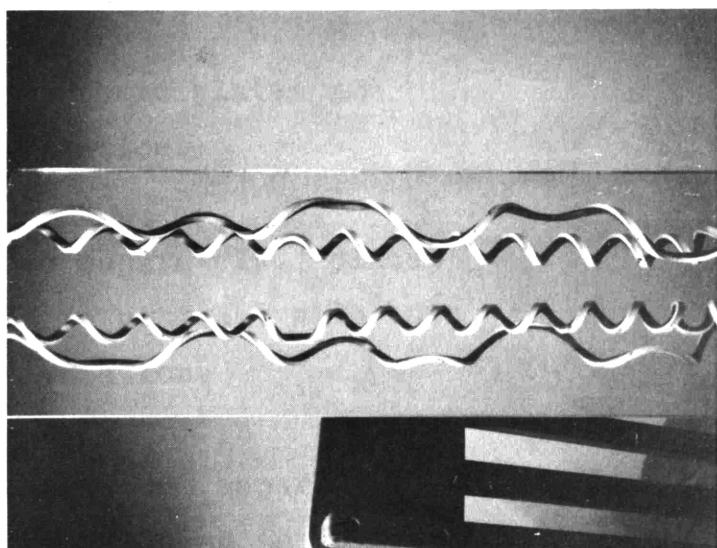
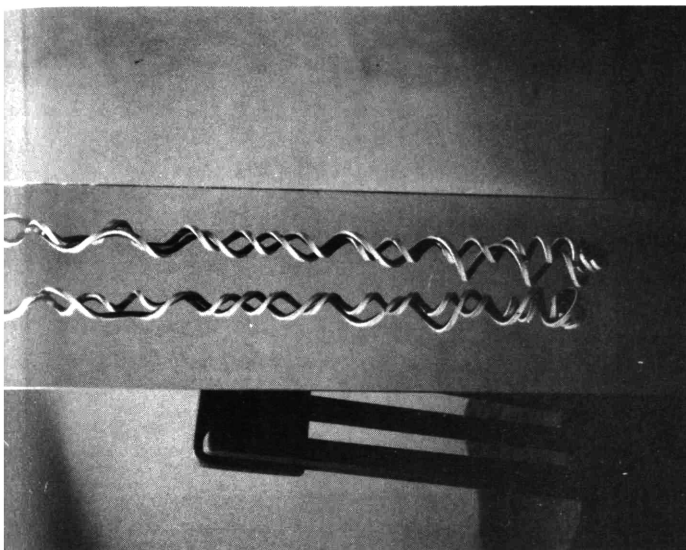


D.



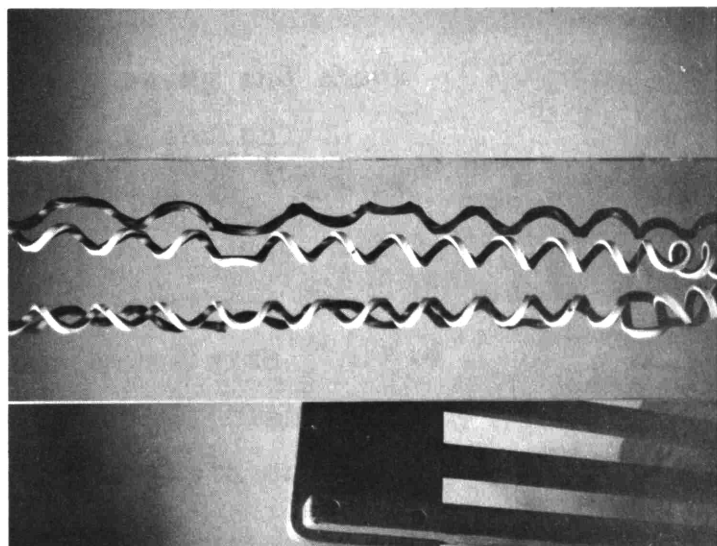
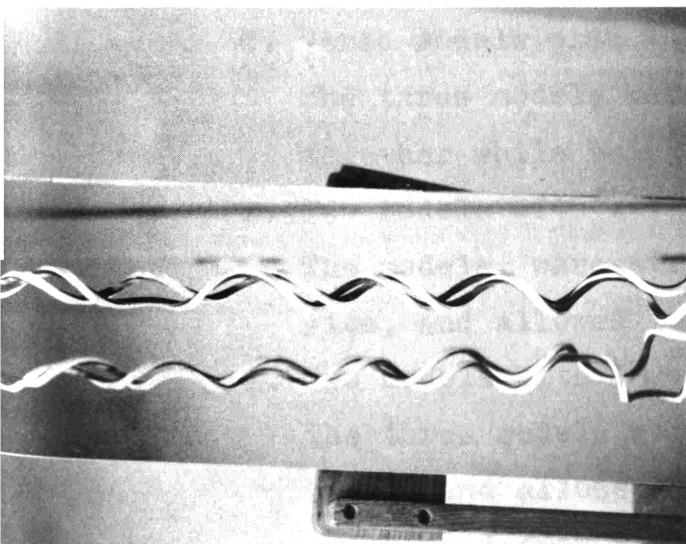
I.

L.



H.

K.



G.

J.

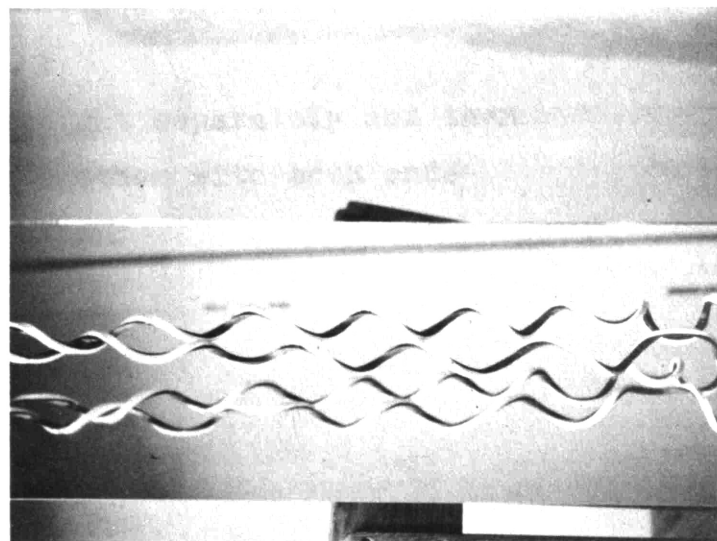
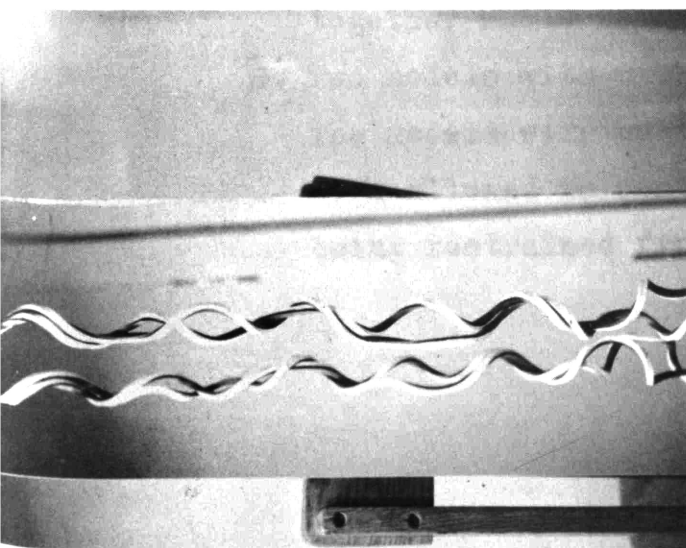


PHOTO PLATES 2 + 3

All the models shown in the two photo plates are approximately square in cross section.

A. Three models with $\Delta L/L = .3$.

The models were straightened separately, placed side by side, then allowed to contract with both ends being restrained from rotation.

B. Three models with $\Delta L/L = .3$.

The three models were stretched out separately, placed side by side, and then allowed to contract, both ends being restrained from rotation. The models are shown hanging under their own weight.

C. Three models with $\Delta L/L = .3$.

The three models were randomly swung and shook together while being held at one end only.

D. Two models with $\Delta L/L = .3$ and one model with $\Delta L/L = .4$.

The models were straightened out, laid side by side, and allowed to contract together.

E. Two models with $\Delta L/L = .3$ and one model with $\Delta L/L = .4$.

The three models were straightened, laid side by side, and allowed to contract, both ends being restrained from rotation.

F. Two models with $\Delta L/L = .3$ and one model with $\Delta L/L = .4$.

The three models were randomly swung and shook together while being held at one end only.

G. Two models with $\Delta L/L = .3$.

The models were pulled straight separately and then were allowed to contract together with both ends being restrained from rotation.

H. Two models with $\Delta L/L = .3$.

The two models were pulled out straight separately, then allowed to contract together with both ends restrained from rotating.

I. One model with $\Delta L/L = .3$ and one model with $\Delta L/L = .4$.

The models were entwined randomly.

J. Two models with $\Delta L/L = .3$.

The models were separated and stretched out. They were then allowed to contract separately with both ends restrained from rotation. They were then pushed close together and allowed to hang freely.

K. Two models with $\Delta L/L = .4$.

These were treated the same as the one in J.

L. One model with $\Delta L/L = .3$ and one model with $\Delta L/L = .4$.

These were treated the same as the models in J.

BIBLIOGRAPHY

1. Brand, R.H., and Backer, Stanley, TEXTILE RESEARCH JOURNAL 32, 39 (1962).
2. Hicks, Elija M., Ryan, James F., Jr., Taylor, Robert B., and Tichenor, Robert L., TEXTILE RESEARCH JOURNAL 30, 675 (1960).
3. Horio, M. and Kondo, T., TEXTILE RESEARCH JOURNAL 23, 373 (1953).
4. Sisson, Wayne A., TEXTILE RESEARCH JOURNAL 30, 153 (1960).
5. Sisson, Wayne A. and Morehead, F.F., TEXTILE RESEARCH JOURNAL 23, 152 (1953).